



## Shielding of uncharged and charged radiation of $\text{PbO-B}_2\text{O}_3-\text{SiO}_2-\text{Na}_2\text{O}$ glass system

Kittisak Sriwongsa<sup>1,2</sup>, Punsak Glumglomchit<sup>3\*</sup>, Bussayamas Sualuang<sup>3</sup>, Punnawich Arunoros<sup>3</sup>,  
Maysinee Pansuay<sup>3</sup>, Sunantasak Ravangvong<sup>4</sup> and Chumphon Khobkham<sup>5</sup>

<sup>1</sup>Lecturers responsible for Bachelor of Education Program in Physics, Faculty of Education, Silpakorn University, Nakhon Pathom, 73000, Thailand

<sup>2</sup>The demonstration school of Silpakorn University, Nakhon Pathom, 73000, Thailand

<sup>3</sup>Huahin Vitthayalai School, Hua-Hin, Prachuap Khiri Khan, 77110, Thailand

<sup>4</sup>Division of Science and Technology, Faculty of Science and Technology, Phetchaburi Rajabhat University, Phetchaburi, 76000, Thailand

<sup>5</sup>Faculty of Engineering, Thonburi University, Bangkok, 10160 Thailand

\* Corresponding author. E-mail address: Punsakk@gmail.com

Received: 19 April 2021; Revised: 12 May 2021; Accepted: 19 May 2021

### Abstract

The aim of this research to study uncharged and charged radiation attenuation properties of  $x\text{PbO-20SiO}_2-10\text{Na}_2\text{O-(70-x)B}_2\text{O}_3$  glass system where  $x = 20, 30, 40, 50$  and  $60$  mol %. Uncharged radiation has been simulated mass attenuation coefficient ( $\mu_m$ ), effective atomic number ( $Z_{\text{eff}}$ ), effective electron density ( $N_{\text{el}}$ ), half value layer (HVL), mean free path (MFP) and build-up factors (BFs) while parameters of charged radiations as alpha ( $\text{He}^{2+}$ ) and proton ( $\text{H}^+$ ) particles have been calculated attenuation properties. The  $\mu_m$ ,  $Z_{\text{eff}}$ ,  $N_{\text{el}}$ , HVL and MFP values were derived from WinXCom program at energy ranging  $1-10^8$  keV. BFs values were determined using geometrical progression (G-P) fitting method for energy ranging 0.015–15 MeV at deep penetration 1–40 mfp (mean free path). While the alpha ( $\text{He}^{2+}$ ) and proton ( $\text{H}^+$ ) particles attenuation properties were simulated from the SRIM software at energy ranging 0.01–10 MeV. The results reported that  $60\text{PbO-20SiO}_2-10\text{Na}_2\text{O-10B}_2\text{O}_3$  glass sample was excellent glass in terms of shielding for uncharged and charged radiation. The results of this research can be useful for variation radiation shielding purpose.

**Keywords:** Uncharged radiation, Charged radiation, Radiation shielding

### Introduction

The development glasses containing heavy metal oxides (HMO) were intended for ionizing radiation shielding. The effective of radiation shielding glasses depend on chemical composition used for glasses (Kaur, Singh & Anand, 2015; Rammah, Al-Buriah & Abouhaswa, 2020; Rammah et al., 2020; Rammah et al., 2020; Olarinoye et al., 2020; Sayyed et al., 2018; Elazoumi et al., 2018). When these glasses are actually applied to specific area, it is necessary to examine the physical and mechanical characteristics of the glass. Ionizing radiation is divided into charged and uncharged radiations, whereas the important in radiation shielding engineering is the interaction which occurs between neutron or photon with a medium (Mahmoud, El-Khatib, Halbas & El-Sharkawy, 2020; El-Sharkawy et al., 2020; Al-Buriah, & Rammah 2019; El-Agawany et al., 2019; Rammah et al., 2018; Sayyed, 2016; Kavaz et al., 2019; Rammah et al., 2021; Sayyed, 2016; El-Bashir, Sayyed, Zaid & Matori, 2017). Therefore, to study against radiation shielding properties of glass, it is necessary to study the parameters of neutron and photon (Rammah et al., 2020;

Rammah et al., 2021; Sayyed, 2016; El-Bashir, Sayyed, Zaid & Matori, 2017; Sayyed et al., 2019; Issa et al., 2019).

The excellent glass materials for photons shielding requires high density and atomic number elemental composition and large mass attenuation coefficients, such as  $\text{PbO}$ ,  $\text{Bi}_2\text{O}_3$ ,  $\text{WO}_3$ , and  $\text{BaO}$ . Whereas glasses for against neutron requires good neutron absorbing elementals composition, such as  $\text{B}$  and  $\text{H}$ .  $\text{PbO}$  as HMO is commonly used for radiation shielding glasses due to it has high density and high atomic number (Chanthima et al., 2011). Therefore,  $\text{Pb}^{2+}$  structure in glass network has been extensively analyzed (Rabinovich, 1976; Witke et al., 1996; Chakradhar, Murali & Rao, 1998; Leventhal & Bray, 2012; Mydlar, Kreidl, Hendren & Clayton, 1970; Dupree, Ford & Holland, 1987; Meera, Sood, Chandrabbas & Ramakrishna, 1990; Meera & Ramakrishna, 1993; Akasaka, Yasui & Nanba, 1993; Hubert, Harder, Mosel & Witke, 1997). At 25–45 mol%,  $\text{PbO}$  will behave network modifier but at 50–60 mol%, it will behave glass network former. Moreover,  $\text{PbO}$  is exhibited very good mechanical, thermal and electrical properties (Pisarska, 2009). Borate ( $\text{B}_2\text{O}_3$ ) wildly used for glass network former, due to it shown good radiation shielding properties (Singh, Singh, Singh & Singh, 2006; Singh, Singh, Singh & Singh, 2004; Singh et al., 2002).

The objective of this work to study the ionizing radiation shielding properties of  $x\text{PbO}-20\text{SiO}_2-10\text{Na}_2\text{O}-(70-x)\text{B}_2\text{O}_3$  glass system where  $x = 20, 30, 40, 50$  and  $60$  mol % (El-Kameesy et al., 2019). The ionizing radiation shielding properties of glass system have been studied in two aspects as uncharged and charged radiation. The parameters studying of uncharged radiation are included mass attenuation coefficient ( $\mu_m$ ), effective atomic number ( $Z_{\text{eff}}$ ), effective electron density ( $N_{\text{el}}$ ), half value layer (HVL), mean free path (MFP) and build-up factors (BFs) while parameters of charged radiation as alpha and proton have been calculated attenuation properties. The  $\mu_m$ ,  $Z_{\text{eff}}$ ,  $N_{\text{el}}$ , HVL and MFP values were derived from WinXCom program at energy ranging  $1-10^8$  keV. BFs values were determined using geometrical progression (G-P) fitting method for energy ranging 0.015–15 MeV at deep penetration 1–40 mfp (mean free path). While the alpha and proton attenuation properties were derived from the SRIM software at energy ranging 0.01–10 MeV.

## Methods and Materials

### 1. Glass samples

This work, the composition chemical and code of glass samples in formula  $x\text{PbO}-20\text{SiO}_2-10\text{Na}_2\text{O}-(70-x)\text{B}_2\text{O}_3$  glass system where  $x = 20, 30, 40, 50$  and  $60$  mol % were exhibited in Table 1 (El-Kameesy et al., 2019).

**Table 1** Chemical composition and code of glass system (El-Kameesy et al., 2019)

Code	Composition (mol%)			
	$\text{PbO}$	$\text{SiO}_2$	$\text{Na}_2\text{O}$	$\text{B}_2\text{O}_3$
PbSiNaB1	20	20	10	50
PbSiNaB2	30	20	10	40
PbSiNaB3	40	20	10	30

**Table 1** (Cont.)

Code	Composition (mol%)			
	PbO	SiO <sub>2</sub>	Na <sub>2</sub> O	B <sub>2</sub> O <sub>3</sub>
PbSiNaB4	50	20	10	20
PbSiNaB5	60	20	10	10

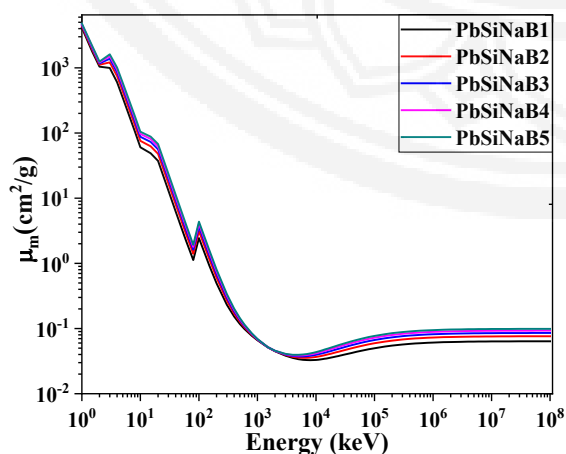
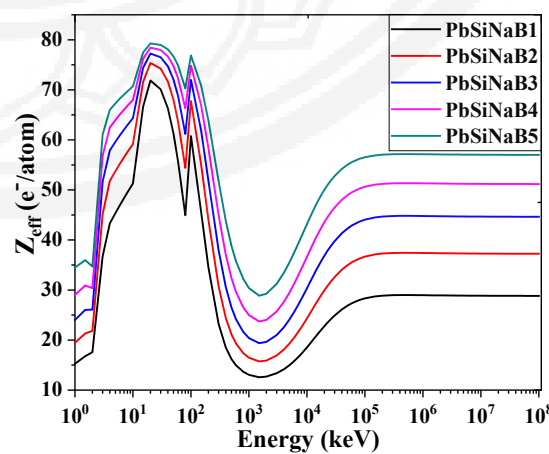
## 2. Uncharged and charged radiation shielding properties

In this context, for PbSiNaB glasses, the important parameters for uncharged radiation shielding parameters such as  $\mu_m$ ,  $Z_{eff}$ ,  $N_{el}$ , HVL, MFP were computed by WinXcom program while BFs were determined using geometrical progression (G-P) fitting method. Charged radiation (proton and alpha particles) interaction parameters were simulated by SRIM software. All parameters have been evaluated as in formerly reports (Kaur, Singh & Anand, 2015; Rammah, Al-Buriahi & Abouhaswa, 2020; Rammah et al., 2020; Rammah et al., 2020; Olarinoye et al., 2020; Sayyed et al., 2018; Mahmoud, El-Khatib, Halbas & El-Sharkawy, 2020; El-Agawany et al., 2019; El-Bashir, Sayyed, Zaid & Matori, 2017; Agar et al., 2019; Kilicoglu et al., 2019; Mhareb et al., 2012; Issa et al., 2020).

## Results and Discussion

### 1. Uncharged radiation shielding properties

The  $\mu_m$  value for  $xPbO-20SiO_2-10Na_2O-(70-x)B_2O_3$  ( $x = 20, 30, 40, 50$  and  $60$  mol %) glass system with energy has been exhibited in Figure 1. The  $\mu_m$  values were high at lower energy ranging and decreased rapidly at intermediate energy ranging after that nearly constant at high energy ranging for all glass samples. These events can be explained on basic interaction of photon with medium which photoelectric effect (PE) ( $\propto E^{-3.5}$ ), Compton scattering (CS) ( $\propto E^{-1}$ ) and pair production (PP) ( $\propto \log E$ ) are main interaction, respectively (Issa et al., 2020). The graphs of  $\mu_m$  values were discontinuities in low energy ranging because of M-, L- and K-absorption edges of Pb, Si and Na in glass systems. Moreover,  $\mu_m$  value increased with increasing of Pb content because of Pb (207.2) are large of atomic weight (Intom et al., 2020).

**Figure 1** The  $\mu_m$  VS energy**Figure 2** The  $Z_{eff}$  VS energy

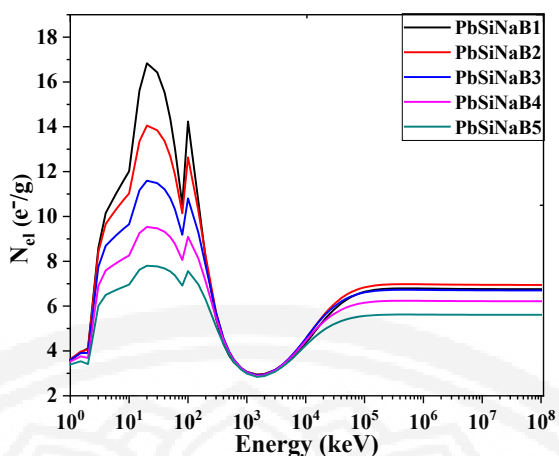


Figure 3 The  $N_{el}$  VS energy

The  $Z_{eff}$  values with energy of glass system has been exhibited in Figure 2. It has been noted that  $Z_{eff}$  value of glass system at energy ranging less than  $10^2$  keV can be discussed on fundamental of absorption edges of Pb (K-edge at 88.00 keV; L-edges at 15.86, 15.20 and 13.04 keV; M-edges at 38.51, 35.54, 30.66, 25.86 and 24.84 keV), Si (K-edge at 18.39 keV) and Na (K-edge at 10.72 keV). At energy ranging of  $10^2$ – $10^3$  keV,  $Z_{eff}$  values for glass system decreases quickly with increasing of energy. During  $10^3$ – $10^5$  keV,  $Z_{eff}$  values increased with increasing of energy. Above  $10^5$  keV,  $Z_{eff}$  values were nearly constant for all glass samples. Among these selected glasses,  $Z_{eff}$  values increased with increasing of PbO content and PbSiNaB5 sample has the highest  $Z_{eff}$  value. This event indicated that PbSiNaB5 sample has the highest probability of interaction between energy with electron in medium (Intom et al., 2020).

Figure 3 exhibits  $N_{el}$  values with energy for glass system. It has been noted that the trend for  $N_{el}$  opposite the trend of  $Z_{eff}$  such as PbSiBaB1 sample has maximum  $N_{el}$  value whereas  $Z_{eff}$  shows minimum value or PbSiNaB5 samples has the lowest of  $N_{el}$  value while  $Z_{eff}$  has the highest value. These events occurred from vacant sites in glass formation of  $B_2O_3$  are filled by PbO atoms which results in decreased  $N_{el}$  of glass sample (Singh, Sharma & Singh, 2018).

Normally, the materials development used for radiation shielding, they should be had low HVL and MFP values because of these two values give rise to a higher probability of radiation interaction with shielding medium. So, these two parameters best discuss about against radiation. Figure 4, and Figure 5 exhibits HVL and MFP of glass samples with energy at  $1$ – $10^8$  keV. It was exhibited that, HVL and MFP values of glass samples were seen very small at  $1$ – $100$  keV and rise quickly with increasing until 7000 keV. After that, HVL and MFP values decreased and becomes almost constant above 800 MeV. This event is according to the cross-section values on energy for various main radiation interaction processes in different energy ranging as mentioned earlier. In addition, HVL and MFP values of glass samples were decreased with increasing in PbO content. It indicated that both values dependent on chemical composition of shielding medium (El-Bashir, Sayyed, Zaid & Matori, 2017; Agar et al., 2019; Issa et al., 2020) and PbSiNaB5 was excellent radiation shielding glass compared with the other glass samples in this research.

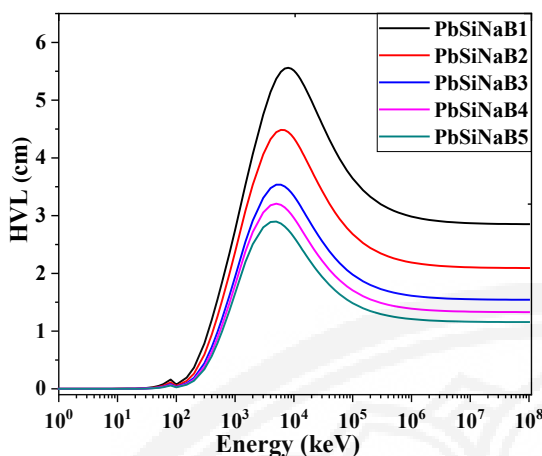


Figure 4 The HVL VS energy

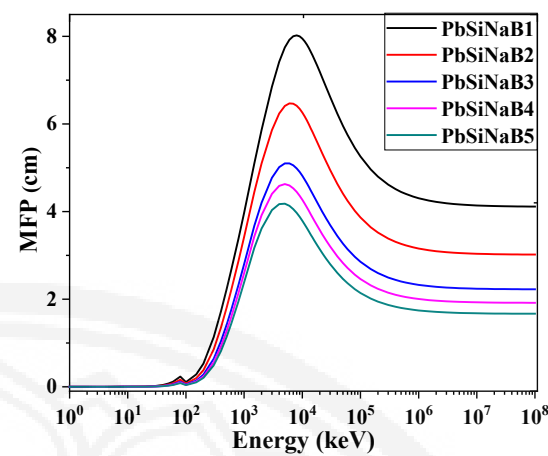
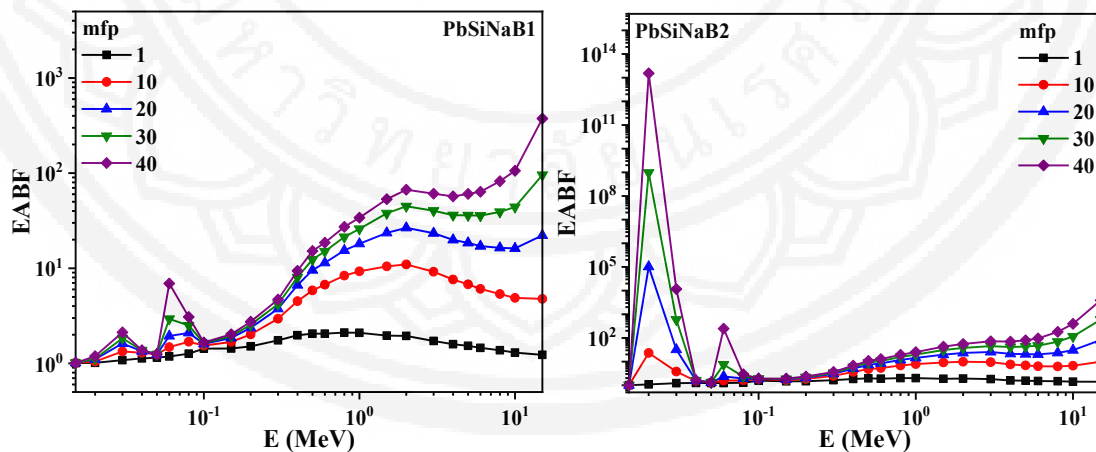


Figure 5 The MFP VS energy

Buildup factors (BFs) is value to explain the absorption of radiation in medium and air which composed energy absorption buildup factor (EABF) and exposure buildup factor (EBF). Figure 6 and 7 shows until 40 mfp of the simulated EABF and EBF within energy 0.015–15 MeV. At low energy ranging, BFs values are low because of photons were absorbed as PE is main mechanism superiority and these ranging shown peaks due to absorption edge (K-edge) of each element which mentioned earlier (El-Agawany et al., 2019; Rammah et al., 2021). Beyond  $10^{-1}$  MeV EABF and EBF values increased again because of photons multiple scattering and occurred accumulated of photon as CS is main process (Olarinoye et al., 2020; El-Agawany et al., 2019). In addition, EABF and EBF values are maxima which dependent on penetration depth (PD). It is clear that EABF and EBF values of results of glass system decrease with increasing PbO content due to the replacement of  $B_2O_3$  by PbO content. This result suggested that PbSiNaB<sub>5</sub> sample which has lowest EABF and EBF values is superior radiation shielding.



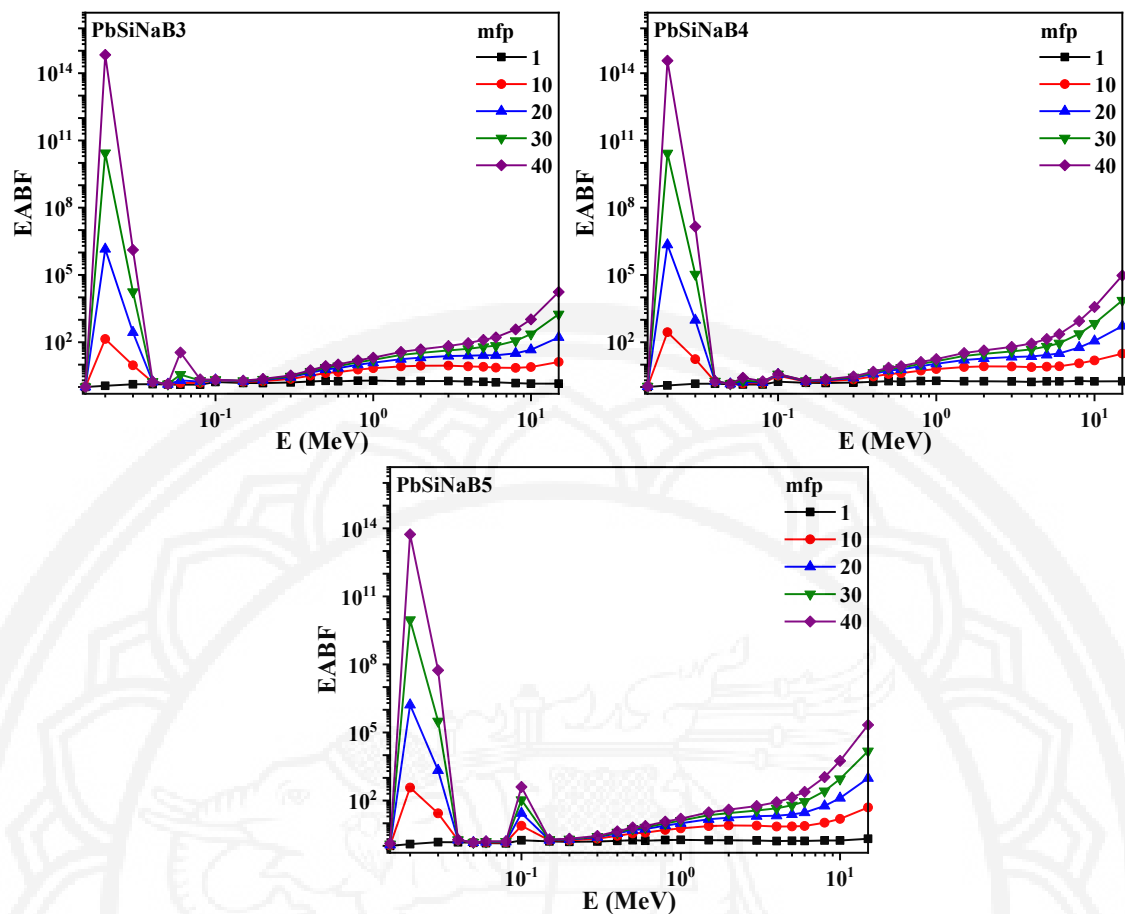
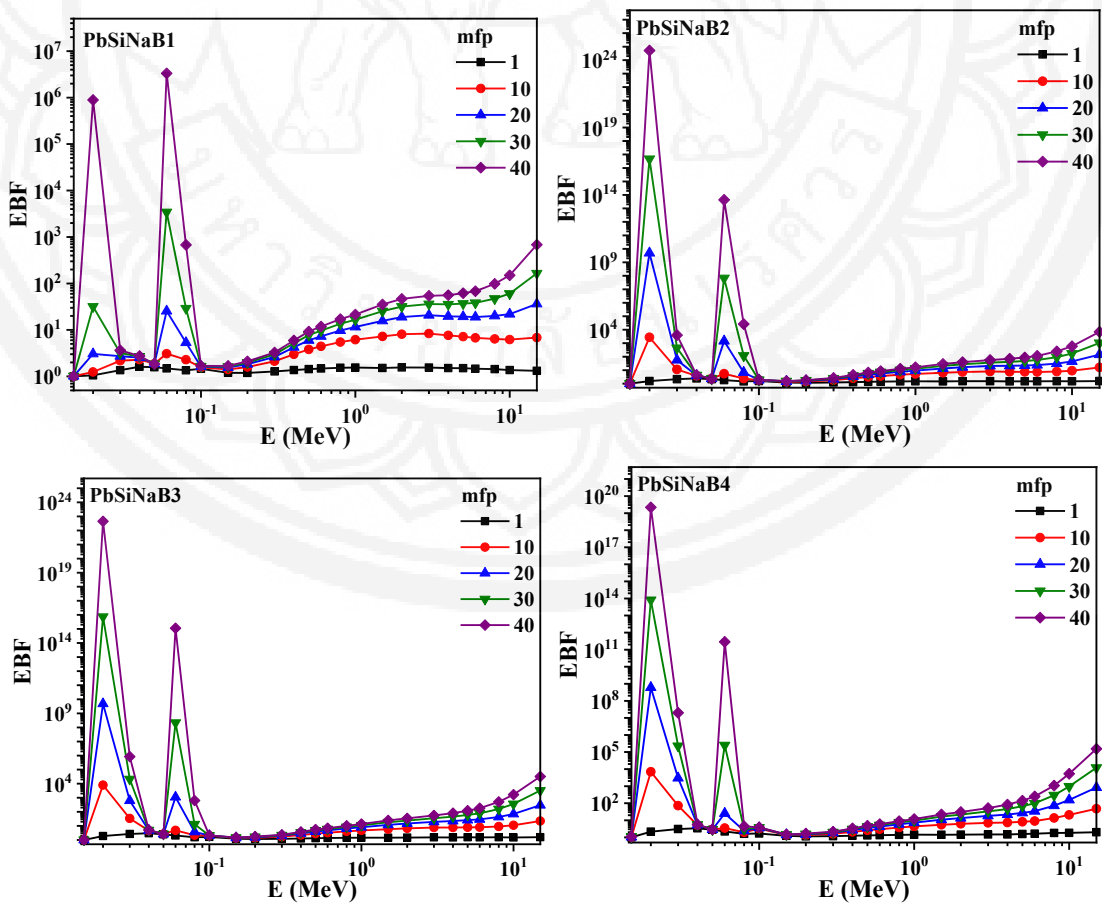
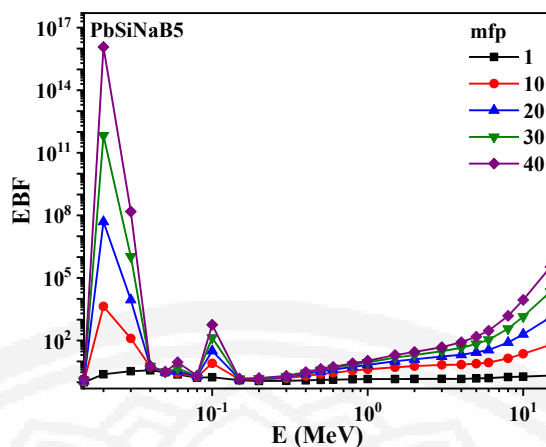


Figure 6 EABF of glass system VS energy from 0.015–15 MeV at 1–40 mfp





**Figure 7** EBF of glass system VS energy from 0.015–15 MeV at 1–40 mfp

## 2. Charged radiation shielding properties

The stopping power of medium is the loss of energy from collision and radiative by charged particles per unit path length which the main process is the collision between particles and atomic electrons. Mass stopping power (MSP) refers to the loss energy by radiation in unit distance per unit density (MeV/g/cm<sup>3</sup>). It can determine from the SRIM program which estimates the MSP and ion range (PR) using the quantum mechanical treatment of ion atom collision (El-Agawany et al., 2019).

The mass stopping powers (MSP) is value to discusses the rate of kinetic energy ( $E_k$ ) loss of ionizing particle and this value is important using determine radiation stopping property of medium (Issa et al., 2019). For charged particles (Except electrons) total mass stopping powers (TMSP) is caused by electronic and nuclear collisions in medium. As a result of this collision, the loss of kinetic energy occurs. Finally, electrically charged particles lose all kinetic energy at a certain depth within the medium through which the particle passes. The TMSP values for glass system have been estimated using SRIM program and results have been exhibited in Figure 9 (a and b). The results of glass system exhibited that TMSP value increase with increasing energy at 0.01–10 MeV for proton and 0.01–10 MeV for alpha after that decrease with increasing energy. Also, the result reported that PbSiNaB5 glass sample has the lowest values of proton and alpha TMSP, respectively. Projected range (PR) values show the mean value of the depth at which proton or alpha would penetrate slowing down to rest. The medium with the lowest PR value requested the excellent for radiation shielding (Issa et al., 2019; Kilicoglu et al., 2019; Mhareb et al., 2012). Figure 10 (a and b) exhibited PR value of glass system and it found that the lowest proton and alpha PR values belong to PbSiNaB5. The results indicated that PbSiNaB5 has the best radiation shielding for H<sup>+1</sup> and He<sup>+2</sup> protection.

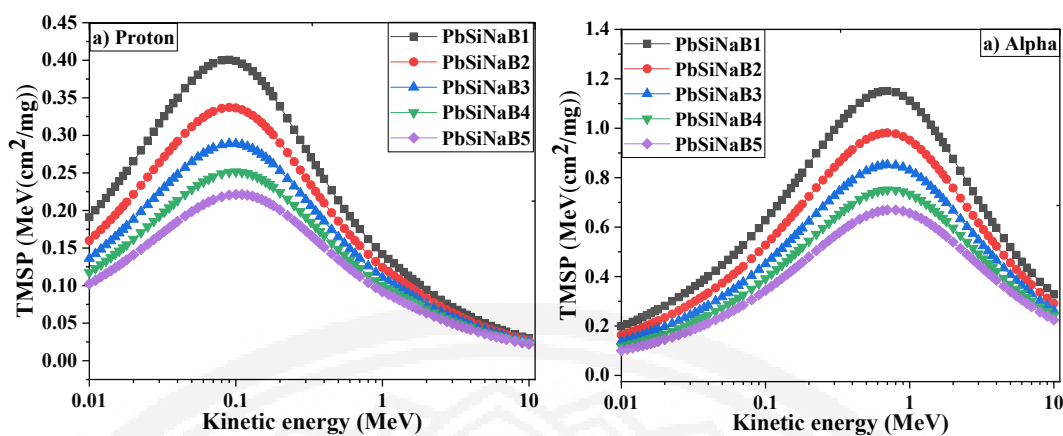


**Figure 8** Total mass stopping powers VS energy of glass system for: a) proton; b) alpha shielding properties

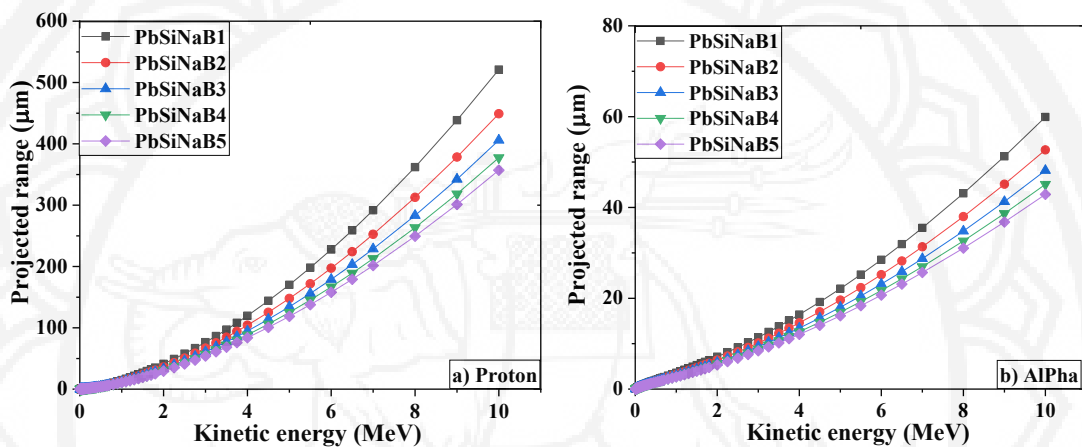


**Figure 9** Projected range VS energy of glass system for: a) proton; b) alpha shielding properties

### Conclusion and Suggestions

The glass system of  $x\text{PbO}-20\text{SiO}_2-10\text{Na}_2\text{O}-(70-x)\text{B}_2\text{O}_3$  where  $x = 20, 30, 40, 50$  and  $60$  mol % was studied the ionizing radiation shielding properties. The ionizing radiation shielding properties of glass system are studied in two aspects as uncharged and charged radiations. The parameters studying of uncharged radiations are included  $\mu_m$ ,  $Z_{\text{eff}}$ ,  $N_{\text{el}}$ , HVL, MFP and BFs while parameters of charged radiations as alpha and proton are calculated attenuation properties. The results reported that the  $60\text{PbO}-20\text{SiO}_2-10\text{Na}_2\text{O}-10\text{B}_2\text{O}_3$  glass sample is the best for uncharged and charged radiations shielding.

### Acknowledgments

The authors thank you to Phetchaburi Rajabhat University, Thailand for support this article.



## References

Agar, O., Kavaz, E., Altunsoy, E. E., Kilicoglu, O., Tekin, H. O., Sayyed, M. I., ... Tarhan, N. (2019).  $\text{Er}_2\text{O}_3$  effects on photon and neutron shielding properties of  $\text{TeO}_2\text{--Li}_2\text{O}\text{--ZnO}\text{--Nb}_2\text{O}_5$  glass system. *Results in physics*, 13, 102277.

Akasaki, Y., Yasui, I., & Nanba, T. (1993). Network structure of  $\text{RO}_x\text{B}_2\text{O}_3$  glasses. *Physics and chemistry of glasses*, 34(6), 232–237.

Al-Buriah, M. S., & Rammah, Y. S. (2019). Electronic polarizability, dielectric, and gamma-ray shielding properties of some tellurite-based glasses. *Applied physics A-materials science & processing*, 125(678), 1–9.

Chakradhar, R. P. S., Murali, A., & Rao, J. L. (1998). Electron paramagnetic resonance and optical absorption studies of  $\text{Cu}^{2+}$  ions in alkali barium borate glasses. *Journal of alloys and compounds*, 265, 29–37.

Chanthima, N., Kaewkhao, J., Kedkaew, C., Chewpraditkul, W., Pokaipisit, A., & Limsuwan, P. (2011). Study on Interaction of  $\text{Bi}_2\text{O}_3$ ,  $\text{PbO}$  and  $\text{BaO}$  in silicate glass system at 662 keV for development of gamma-rays shielding materials. *Progress in nuclear science and technology*, 1, 106–109.

Dupree, R., Ford, N., & Holland, D. (1987). An examination of the  $\text{Si-29}$  environment in the  $\text{PbO-SiO}_2$  system by magic angle spinning nuclear magnetic resonance. *Physics and chemistry of glasses*, 28(2), 78–84.

Elazoumi, S. H., Sidek, H. A. A., Rammah, Y. S., El-Mallawany, R., Halimah, M. K., Matori, K., & Zaid, M. H. M. (2018). Effect of  $\text{PbO}$  on optical properties of tellurite glass. *Results in physics*, 8, 16–25.

El-Agawany, F. I., Kavaz, E., PeriŞanoğlu, U., Al-Buriah, M. S., & Rammah, Y. S. (2019).  $\text{Sm}_2\text{O}_3$  effects on mass stopping power/projected range and nuclear shielding characteristics of  $\text{TeO}_2\text{--ZnO}$  glass systems. *Applied physics A-materials science & processing*, 125(838), 1–12.

El-Bashir, B. O., Sayyed, M. I., Zaid, M. H. M., & Matori, K. A. (2017). Comprehensive study on physical, elastic and shielding properties of ternary  $\text{BaO-Bi}_2\text{O}_3\text{--P}_2\text{O}_5$  glasses as a potent radiation shielding material. *Journal of non-crystalline solids*, 468, 92–99.

El-Kameesy, S. U., El-Zaiat, S. Y., Youssef, G. M., Saudi, H. A., El-Fiki, S. A., & Abu-raia, W. A. (2019). Linear optical properties of  $x\text{PbO-20SiO}_2\text{--10Na}_2\text{O-(70-x)B}_2\text{O}_3$  glass system. *Sillicon*, 11(18), 1505–1515.

El-Sharkawy, R. M., Shaaban, K. S., Elsaman, R., Allam, E. A., El-Taher, A., & Mahmoud, M. E. (2020). Investigation of mechanical and radiation shielding characteristics of novel glass systems with the composition  $x\text{NiO-20ZnO-60B}_2\text{O}_3\text{--(20-x)CdO}$  based on nanometal oxides. *Journal of non-crystalline solids*, 528, 119754.

Hubert, T., Harder, U., Mosel, G., & Witke, K. (1997). Borate glasses, crystals and melts. In: Wright, A. C., Feller, S. A., Hannon, A. C. (eds) 2nd International Conference Borate glasses, crystals and melts. *Society of Glass Technology Sheffield*, 156–163.

Intom, S., Kalkornsuraprancee, E., Johns, J., Kaewjaeng, S., Kothan, S., Hongtong, W., ... Kaewkhao, J. (2020). Mechanical and radiation shielding properties of flexible material based on natural rubber/ $\text{Bi}_2\text{O}_3$  composites. *Radiation physics and chemistry*, 172, 108772.



Issa, S. A. M., Rashad, M., Zakaly, H. M. H., Tekin, H. O., & Abouhaswa, A. S. (2020).  $\text{Nb}_2\text{O}_5\text{--Li}_2\text{O}\text{--Bi}_2\text{O}_3\text{--B}_2\text{O}_3$  novel glassy system: evaluation of optical, mechanical, and gamma shielding parameters. *Journal of materials science: materials in electronics*, 31(24), 1–18.

Issa, S. A. M., Tekin, H.O., Elsaman, R., Kilicoglu, O., Saddeek, Y. B., & Sayyed, M. I. (2019). Radiation shielding and mechanical properties of  $\text{Al}_2\text{O}_3\text{--Na}_2\text{O}\text{--B}_2\text{O}_3\text{--Bi}_2\text{O}_3$  glasses using MCNPX Monte Carlo code. *Materials chemistry and physics*, 223, 209–219.

Kaur, K., Singh, K. J., & Anand, V. (2015). Correlation of gamma ray shielding and structural properties of  $\text{PbO}\text{--BaO}\text{--P}_2\text{O}_5$  glass system. *Nuclear engineering and design*, 285, 31–38.

Kavaz, E., Ekinci, N., Tekin, H. O., Sayyed, M. I., Aygün, B., & PeriŞanoğlu, U. (2019). Estimation of gamma radiation shielding qualification of newly developed glasses by using WinXCOM and MCNPX code. *Progress in nuclear energy*, 115, 12–20.

Kilicoglu, O., Altunsoy, E. E., Agar, O., Kamislioglu, M., Sayyed, M. I., Tekin, H. O., & Tarhan, N. (2019). Synergistic effect of  $\text{La}_2\text{O}_3$  on mass stopping power (MSP)/projected range (PR) and nuclear radiation shielding abilities of silicate glasses. *Results in physics*, 4, 102424.

Leventhal, M., & Bray, P. J. (2012). Nuclear Magnetic Resonance Investigation of Compounds and Glasses in Systems  $\text{PbO}\text{--B}_2\text{O}_3$  and  $\text{PbO}\text{--SiO}_2$ . *Physics and chemistry of glasses*, 6, 113–125.

Mahmoud, M. E., El-Khatib, A. M., Halbas, A. M., & El-Sharkawy, R. M. (2020). Investigation of physical, mechanical and gamma-ray shielding properties using ceramic tiles incorporated with powdered lead oxide. *Ceramics international*, 46, 15686–15694.

Meera, B. N., & Ramakrishna, J. (1993). Raman spectral studies of borate glasses. *Journal of non-crystalline solids*, 159, 1–12.

Meera, B. N., Sood, A. K., Chandrabbas, N., & Ramakrishna, J. (1990). Raman study of lead borate glasses. *Journal of non-crystalline solids*, 126, 224–230.

Mhareb, M. H. A., Alajerami, Y. S. M., Dwaikat, N., Al-Buriahi, M. S., Alqahtani, M., Alshahri, F., ... Sayyed, M. I. (2012). Investigation of photon, neutron and proton shielding features of  $\text{H}_3\text{BO}_3\text{--ZnO}\text{--Na}_2\text{O}\text{--BaO}$  glass system. *Nuclear engineering and technology*, 53, 949–959.

Mydlar, M. F., Kreidl, N. J., Hendren, J. K., & Clayton, G. T. (1970). X-ray diffraction study of lead silicate glasses. *Physics and chemistry of glasses*, 11, 196–201.

Olarinoye, I. O., El-Agawany, F. I., El-Adawy, A., El-Sayed, Y., & Rammah, Y. S. (2020). Mechanical features alpha particles photon proton and neutron interaction parameters of  $\text{TeO}_2\text{--V}_2\text{O}_3\text{--MoO}_3$  semiconductor glasses. *Ceramics international*, 46(14), 23134–23144.

Pisarska, J., (2009). Luminescence behaviour of  $\text{Dy}^{3+}$  ions in lead borate glasses. *Optical materials*, 31, 1784–1786.

Rabinovich, E. M. (1976). Lead in glasses. *Journal of materials science*, 11, 925–948.

Rammah, Y. S., Al-Buriahi, M. S., & Abouhaswa, A. S. (2020).  $\text{B}_2\text{O}_3\text{--BaCO}_3\text{--Li}_2\text{O}_3$  glass system doped with  $\text{Co}_3\text{O}_4$ : structure, optical, and radiation shielding properties. *Physica B: physics of condensed matter*, 576, 411717.

Rammah, Y. S., El-Agawany, F. I., Mahmoud, K. A., Novatski, A., & El-Mallawany, R. (2020). Role of  $\text{ZnO}$  on  $\text{TeO}_2\text{--Li}_2\text{O}\text{--ZnO}$  glasses for optical and nuclear radiation shielding applications utilizing MCNP5 simulations and WinXCOM program. *Journal of non-crystalline solids*, 544, 120162.



Rammah, Y. S., Kilic, G., El-Mallawany, R., Issever, U. G., & El-Agawany, F.I. (2020). Investigation of optical, physical, and gamma-ray shielding features of novel vanadyl boro-phosphate glasses. *Journal of non-crystalline solids*, 533, 119905.

Rammah, Y. S., Sayyed, M. I., Ali, A. A., Tekin, H. O., & El-Mallawany, R. (2018). Optical properties and gamma shielding features of bismuth borate glasses. *Applied physics A-materials science & processing*, 124(832), 1–9.

Rammah, Y. S., Tekin, H. O., Sriwunkum, C., Olarinoye, I., Alalawi, A., Al-Buriahi, M. S., ... Tonguc, B. T. (2021). Investigations on borate glasses within SBC-B<sub>x</sub> system for gamma-ray shielding applications. *Nuclear engineering and technology*, 53(1), 282–293.

Sayyed, M. I. (2016). Bismuth modified shielding properties of zinc boro-tellurite glasses. *Journal of alloys and compounds*, 688, 111–117.

Sayyed, M. I. (2016). Investigations of gamma ray and fast neutron shielding properties of tellurite glasses with different oxide compositions. *Canadian journal of physics*, 94(11), 1133–1137.

Sayyed, M. I., Kaky, K. M., Gaikwad, D. K., Agar, O., Gawai, U. P., & Baki, S. O. (2019). Physical, structural, optical and gamma radiation shielding properties of borate glasses containing heavy metals (Bi<sub>2</sub>O<sub>3</sub>/MoO<sub>3</sub>). *Journal of non-crystalline solids*, 507, 30–37.

Sayyed, M. I., Tekin, H. O., Kiliçoglu, O., Agar, O., & Zaid, M. H. M. (2018). Shielding features of concrete types containing sepiolite mineral: comprehensive study on experimental, XCOM and MCNPX results. *Results in physics*, 11, 40–45.

Singh, H., Sharma, J., & Singh, T. (2018). Extensive investigations of photon interaction properties for Zn<sub>x</sub>Te<sub>100-x</sub> alloys. *Nuclear engineering and technology*, 50, 1364–1371.

Singh, K., Singh, H., Sharma, V., Nathuram, R., Khanna, A., Kumar, R., ... Sahota, H. S. (2002). Gamma-ray attenuation coefficients in bismuth borate glasses. *Nuclear instruments and methods in physics research B*, 194, 1–6.

Singh, N., Singh, K. J., Singh, K., & Singh, H. (2004). Comparative study of lead borate and bismuth lead borate glass systems as gamma-radiation shielding materials. *Nuclear instruments and methods in physics research B*, 225, 305–309.

Singh, N., Singh, K. J., Singh, K., & Singh, H. (2006). Gamma-ray attenuation studies of PbO–BaO–B<sub>2</sub>O<sub>3</sub> glass system. *Radiation measurements*, 41, 84–88.

Witke, K., Harder, U., Willfahrt, M., Hubert, T., & Reich, P. (1996). Vibrational spectroscopic investigations of lead borate and lead aluminoborate glasses. *Glass science and technology*, 69, 143–153.